SLAC-PUB-9663
LCC-0116
March 2003

Short-range dipole wakefields in accelerating structures for the NLC

Karl L.F. Bane*

Stanford Linear Accelerator Center,

Stanford University, Stanford, CA 94309

(Dated: March 4, 2003)

*Work supported by the Department of Energy, contract DE-AC03-76SF00515

I. INTRODUCTION AND CONCLUSION

A knowledge of the short-range wakefields in the accelerating structures of the NLC, particularly those in the main (x-band) linac, is of critical importance for the design of the project. In a linac the short-range longitudinal wakes increase the single bunch energy spread, and the short-range transverse (dipole) wakes, when there are structure misalignments and/or orbit errors, will increase the single bunch projected emittance of the beam.

The numerically obtained short-range longitudinal and dipole wakes of the 206 cell Damped, Detuned Structure (DDS) were presented in Ref. [1]. However, it seems that a parameterization of the short-range wakes in terms of the geometric properties of an accelerating structure, over some useful range of parameters, can be an aid in the design of the NLC. Such a parameterization has been performed for the short-range longitudinal wakes of accelerating structures [2] using a field matching program written by K. Yokoya [3], and in this report we repeat the exercise for the dipole wakes. Note that a similar work has also been performed by Yokoya [4], though our result is in a somewhat simpler form and also includes a dependence on iris thickness.

In conclusion, in this report we do find a simple model that appears to agree with numerical results to within a few percent for constant impedance, disk-loaded structures over a parameter range useful for the NLC: $0.35 \lesssim a/L \lesssim 0.70$ and $0.55 \lesssim g/L \lesssim 0.90$, where a is iris radius, L is structure period, and g is gap length; for wakefield argument (distance parameter) s up to $s/L \approx 0.15$. The model depends strongly on a/L but weakly on g/L. For detuned structures, with cell dimensions that vary within the structure, the structure wake is obtained by averaging the model wakes corresponding to the individual cell geometries.

II. SHORT-RANGE WAKEFIELD

The types of structures we consider are cylindrically symmetric. A driving charge q moves at the speed of light c parallel to and at horizontal offset x_q from the structure axis; a test particle follows at offset x and at distance s behind the driving charge. The particles move near the axis, and thus the longitudinal kick is dominated by monopole fields (azimuthally independent) and the transverse kick by dipole fields. The longitudinal kick experienced by the test particle per unit distance, divided by q, defines the longitudinal wake W_L, and the

transverse kick experienced by the test particle per unit distance, divided by qx_q, defines the transverse wake W_x (see, *e.g.* A. Chao [5]). The Fourier transform of the wakes give the longitudinal and transverse impedances, Z_L and Z_x.

For a bunch with longitudinal (position) distribution λ, the transverse kick, at longitudinal position s, is given by

$$V_x(s) = q \int_{-\infty}^{s} W_x(s - s')x(s')\lambda(s')\, ds' \ , \tag{1}$$

where here q is the charge of the bunch. For a bunch entirely offset by x_q, the normalized kick (kick divided by qx_q) along the bunch (the bunch wake) is

$$\mathcal{W}_x(s) = \int_{-\infty}^{s} W_x(s - s')\lambda(s')\, ds' \ ; \tag{2}$$

the average kick over the entire bunch (the total bunch kick factor) is

$$\mathcal{K}_x(s) = \int_{-\infty}^{\infty} \mathcal{W}_x(s)\lambda(s)\, ds \ . \tag{3}$$

A. Analytical High Frequency Impedance

Let us consider a perfectly conducting, disk-loaded accelerating structure with the geometry given in Fig. 1. Structure parameters are iris radius a, gap g, period L, and cavity radius b (in the short range wakes that we consider, the parameter b will not appear). The high frequency *longitudinal* impedance of such a structure was found by R. Gluckstern, with a modification by Yokoya and Bane, to be given by [6, 7]

$$Z_L(k) = \frac{iZ_0}{\pi k a^2}\left[1 + (1+i)\frac{\alpha(g/L)\, L}{a}\sqrt{\frac{\pi}{kg}}\right]^{-1} \qquad [k \text{ large}] \quad , \tag{4}$$

with k the wave number and $Z_0 = 120\pi\Omega$; where the parameter α can be approximated by [7]

$$\alpha(\gamma) \approx 1 - \alpha_1\sqrt{\gamma} - (1 - 2\alpha_1)\gamma \quad , \tag{5}$$

with $\alpha_1 = 0.4648$. If we inverse Fourier transform Eq. 4 we obtain the very short-range wakefield [2]:

$$W_L(s) \approx \frac{Z_0 c}{\pi a^2}\phi(s) \exp\left(\frac{\pi s}{4s_{00}}\right) \operatorname{erfc}\left(\sqrt{\frac{\pi s}{4s_{00}}}\right) \qquad [s \text{ small}] \quad , \tag{6}$$

with $\phi(s)$ the step function [$\phi(s) = 1$ for $s > 0$, 0 for $s < 0$], and

$$s_{00} = \frac{g}{8}\left(\frac{a}{\alpha(g/L)\,L}\right)^2 \quad . \tag{7}$$

A simpler way of writing the short-range wake, one that also has leading order dependence on s consistent with Eq. 4 (*i.e.* up to the $\sqrt{s}$ term), is

$$W_L(s) \approx \frac{Z_0 c}{\pi a^2}\phi(s)\exp\left(-\sqrt{\frac{s}{s_{00}}}\right) \qquad [s \text{ small}] \quad . \tag{8}$$

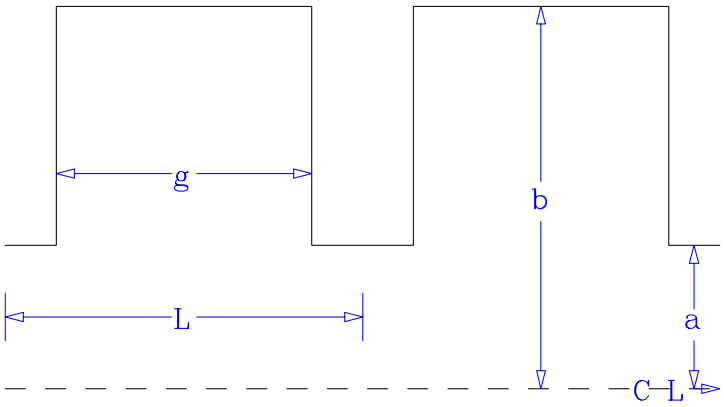

FIG. 1: The geometry of two cells of the structure under consideration.

The high frequency *dipole* impedance of the structure was found by Fedotov, *et al*, to be related to the high frequency monopole impedance in the same simple way as for the resistive wall wake of a cylindrical metallic pipe [8]. That is, at high frequency

$$Z_L^{(1)} = \frac{2}{a^2}Z_L \ , \qquad Z_x = \frac{2}{ka^2}Z_L \qquad [k \text{ large}] \quad , \tag{9}$$

which implies that at short distances

$$W_L^{(1)} = \frac{2}{a^2}W_L \ , \qquad W_x = \frac{2}{a^2}\int_0^s W_L(s')\,ds' \qquad [s \text{ small}] \ , \tag{10}$$

where superscript (1) denotes the longitudinal component of the dipole impedance or wake. Therefore, combining Eq. 8,10, we find that the short range dipole wake becomes

$$W_x(s) = \frac{4Z_0 c s_{00}}{\pi a^4}\phi(s)\left[1 - \left(1 + \sqrt{\frac{s}{s_{00}}}\right)\exp\left(-\sqrt{\frac{s}{s_{00}}}\right)\right] \quad . \tag{11}$$

B. Numerically Obtaining the Short-Range Wakefield

To numerically obtain the short-range dipole wakefield we use a computer program developed by K. Yokoya [3], based on an impedance field matching formalism by H. Henke [9]. The program first finds the impedance of the periodic structure of Fig. 1 (but with $b \to \infty$) by field matching. The impedance, however, is found along a line shifted above the real k axis by a small amount, $Im(k)$, instead of along the real axis itself. This impedance is then inverse Fourier transformed to give the wake W_x, a result that is theoretically independent of $Im(k)$. The wake can be written, for example, as

$$W_x = \frac{2c}{\pi} \int_0^\infty R_x(k) \sin ks \, dk \ , \tag{12}$$

where R_x is the real part of the impedance; or, by using a Kramers-Kronig relation to write R_x in terms of the imaginary part of the impedance X_x, the wake can be written as an integral over X_x. K. Yokoya's program calculates the wake in both ways, as a check on the accuracy of the result. Note that since, at high frequency, the transverse impedance drops one power of k faster than the longitudinal impedance ($R_x \sim k^{-5/2}$), the high frequency behavior is relatively less important than in the longitudinal case.

To see how the shift in integration path is useful, note that normally, on the real k axis, R_x is spiky (a sum of delta functions if we assume perfectly conducting walls), with the density of spikes increasing with increasing frequency, while at the same time X_x similarly becomes a quickly varying function. Along a path above the real axis, however, the impedance (both parts) becomes smoother, and a smooth function is easier to (numerically) inverse Fourier transform. A disadvantage of this method, however, is that the inverse Fourier transform ends up with a wakefield in the form $e^{Im(k)s}F(s)$; at large s the function $F(s)$ becomes very small. For given $Im(k)$ this limits the range in s for which the wakefield can practically be computed.

The method that in the past has been used to find the wakefields for the SLAC linac structure [10] and for that of the NLC main linac [1] involves field matching for the modes (equivalent to finding the impedance on the real axis) for the structure of Fig. 1. The first 100 or so mode frequencies and kick factors are obtained numerically using the computer program TRANSVRS[11]. The rest of the impedance is taken to be given by the so-called Sessler-Vainsteyn (S-V) analytical extension [12]. To see why this extension is important, consider that the density of modes $dn/dk^2 \approx gb/(2\pi)$. For the NLC DDS x-band structure,

$g \approx 7$ mm, $b \approx 10$ mm, and the typical bunch length $\sigma_z = 0.1$ mm. To find the impedance up to $k = 10/\sigma_z$ (100 mm^{-1}) we would need to find $\sim 10^5$ modes, which is not feasible. The advantage of this method over Yokoya's method is that it gives the wake over longer distances s, up to values where coupling between neighboring cells of a structure begins to become important. The disadvantage is that one needs a fine step in frequency to avoid missing modes in the calculation, and that the S-V model, although intuitively understandable, does not have a firm theoretical basis.

The S-V model of impedance is a simple model that combines the power spectrum of a high energy particle with the diffraction of light at the edges of a periodic array of thin, circular mirrors. It is a model that has been used for many years and that seemed to agree reasonably well with the binned and averaged, numerically obtained real part of the impedance over an intermediate frequency range for SLAC and NLC structures. In the dipole case the real part of the impedance is given by

$$R_x = \sum_{n=1}^{nup} \frac{\pi \kappa_{xn}}{c} \delta(k - k_n) + \frac{Z_0 j_{11}^2}{\pi \zeta^2 k a^2 L} \frac{\sqrt{\nu} + 1}{(\nu + 2\sqrt{\nu} + 2)^2} \phi(k - k_N) \quad k > 0 \quad , \tag{13}$$

with k_n, κ_{xn}, mode frequencies and kick factors of the first nup modes; $j_{11} = 3.83$, $\zeta = 0.824$, $\nu = 4a^2 k/(\bar{L}\zeta^2)$, and $\bar{L} = \sqrt{Lg}$. Note that at very high frequencies the correct asymptotic behavior of the impedance, Eq. 4, implies a real part

$$R_x(k) = \frac{2 Z_0 \alpha (g/L)\, L}{\sqrt{\pi} a^5 g^{1/2} k^{5/2}} \qquad [k \to \infty] \quad , \tag{14}$$

whereas, for the S-V model $R_x(k) = (Z_0 j_{11}^2 \zeta \bar{L}^{3/2})/(8\pi a^5 k^{5/2} L)$. We see that the a and k dependence of the S-V model is correct, but the g dependence is not. However, for typical cavities $g/L \approx 1$ and $\bar{L} \approx L$, which implies that $\alpha \approx 0.5$. For such cavities the S-V model asymptotic behavior equals approximately 0.85 times the correct asymptotic behavior.

In example cases (as we will see for the DDS structure discussed below), the resulting wakes of the two calculation methods agree quite well. Finally, for completeness, we should note that the short-range dipole wake, convolved with a smooth bunch shape—the bunch wake $\mathcal{W}_x$—can also be obtained accurately by direct time domain calculations, using a computation method recently developed by Zagorodnov and Weiland[13].

III. RESULTS

As an example, we consider first the impedance of a periodic structure with the dimensions of the average cell in the 206-cell NLC DDS structure. For this cell $a = 4.92$ mm, $g = 6.89$ mm, and $L = 8.75$ mm. The numerically obtained impedance, when $Im(k) = 0.5$ mm^{-1}, is shown in Fig. 2. Shown are R_x (solid line), $|X_x|$ (dashes), and the analytical asymptotic equation, Eq. 4 (dots). [The function X crosses zero and becomes positive near $Re(k) \approx 0.85$ mm^{-1}.] We note that the impedance is indeed smooth. With only ~ 100 calculated points we have characterized the impedance up to $k = 200$ mm^{-1}! We note also that for $Re(k) \gtrsim 5$ mm^{-1} the numerically obtained impedance is in reasonably good agreement with the analytical asymptotic formula. [A deviation for R_x, however, can be seen developing gradually at high frequencies; it is not understood. But, since it is far in the tail of the impedance, the behavior here does not affect the short-range wake result given below.]

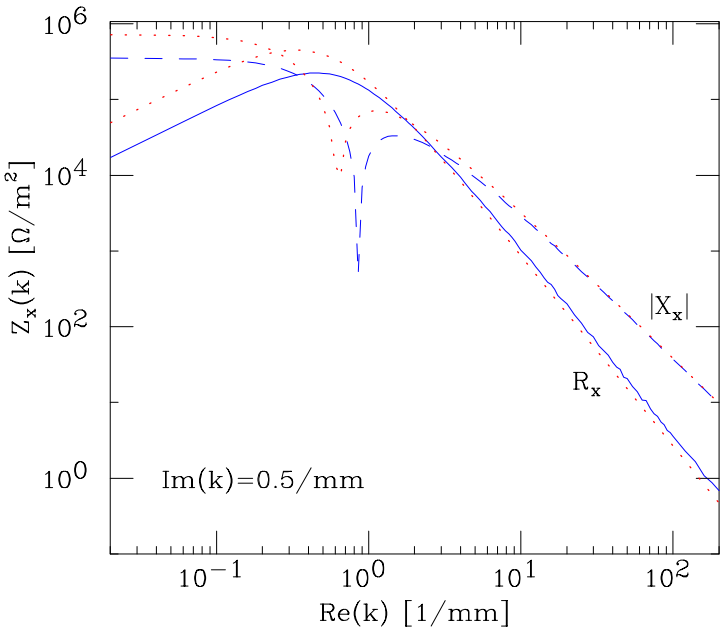

FIG. 2: The impedance for the DDS average cell geometry along a path shifted by $Im(k) = 0.5$ mm^{-1}. Shown are the real part R_x of the impedance (solid) and the absolute value of the imaginary part $|X_x|$ (dashes). The dots display the behavior of the asymptotic solution, Eq. 4.

Performing the inverse Fourier transform of the impedance, Yokoya's program then obtains the short-range wake. The result is shown in Fig. 3 (the solid curve). Note that, whether obtained from R_x or X_x, the wakefield over the range plotted is essentially the

same. Also shown in the figure are the short range asymptotic solutions: Eq. 11 (dashes), and the transverse wake corresponding to Eq. 6 (dots). We note that the numerically obtained wake function is in reasonably good agreement with the analytical result near the origin, and that the analytical wakes seem to approximate the numerical result well up to ~ 0.2 mm. But to estimate how appropriate the asymptotic solutions are for a tracking program we use them to calculate the bunch wake $\mathcal{W}_x$ and the total kick factor $\mathcal{K}_x$ for Gaussian bunches of different lengths, and compare with the results of the numerical wake (see Table I). We see that for the nominal NLC 0.1 mm long bunch, if 10-15% accuracy does not suffice, then the asymptotic solutions are not good enough.

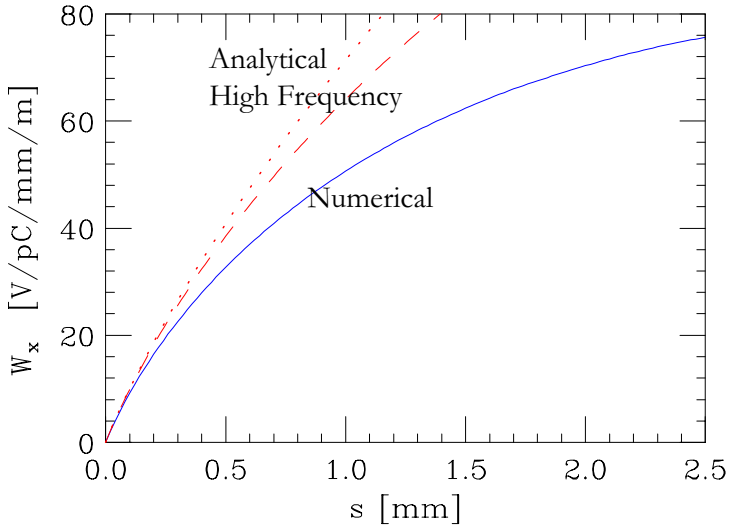

FIG. 3: The wakefield corresponding to Fig. 2 (solid). Also shown are the short range asymptotic solutions: Eq. 11 (dashes), and the transverse wake corresponding to Eq. 6 (dots).

TABLE I: Error in using the asymptotic wakefields (Eq. 11) for calculating bunch wakes for a Gaussian bunch with rms length σ_z: given are the maximum error in the bunch wake $\mathcal{W}_x$ ($-4\sigma_z < s < 4\sigma_z$), and the error in the total kick factor $\mathcal{K}_x$.

$\sigma_z[mm]$	Max($\mathcal{W}_x$ error) [%]	$\mathcal{K}_x$ error [%]
0.05	11	7
0.10	16	9
0.15	20	12

To obtain a fitted wake function that is valid over an expanded parameter regime useful

for NLC studies, we first numerically obtained wakefields on a parameter grid in the region $0.34 \leq a/L \leq 0.69$ and $0.54 \leq g/L \leq 0.89$. Fitting to the numerical results, we find a reasonably good fit over $0 \leq s/L \leq 0.16$ (up to $s = 1.4$ mm for the DDS structure) for a function of the same form as the asymptotic, short-range solution:

$$W_x(s) = \frac{4Z_0 c s_0}{\pi a^4}\phi(s)\left[1 - \left(1 + \sqrt{\frac{s}{s_0}}\right)\exp\left(-\sqrt{\frac{s}{s_0}}\right)\right] , \tag{15}$$

with

$$s_0 = 0.169\frac{a^{1.79}g^{0.38}}{L^{1.17}} . \tag{16}$$

Note that this function has the correct slope at $s = 0^+$, and that the a dependence is similar to the very short-range asymptotic wake, whereas the g dependence is not similar, and is very weak. Fig. 4 shows the individual fitted values of s_0 compared to the value given in Eq. 16, and Fig. 5 shows the agreement of the model to representative numerically obtained wakes. We see that the agreement is reasonably good.

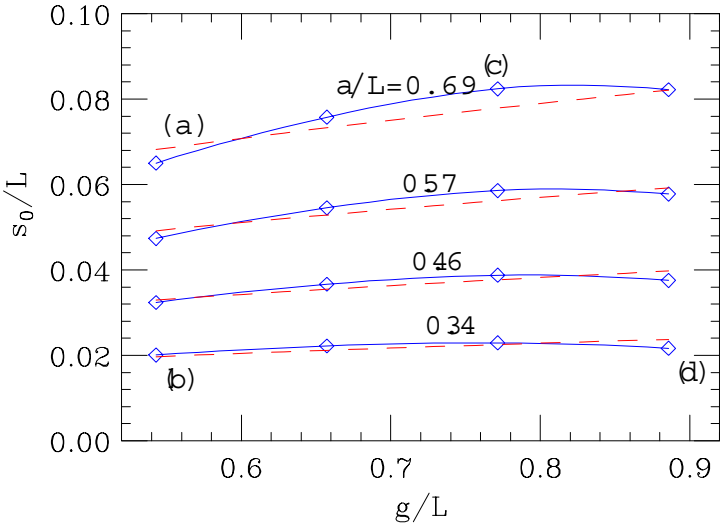

FIG. 4: Results of our parameter study giving the fitted parameter s_0/L *vs.* g/L for four values of a/L. The plotting symbols (the diamonds) give the fits to the numerically obtained wakes, and the dashes display Eq. 15.

A. Examples

For three example structures we compare numerical wakes with the model. First is the DDS structure. It is a 206-cell, x-band structure operating at $2\pi/3$ phase advance. The

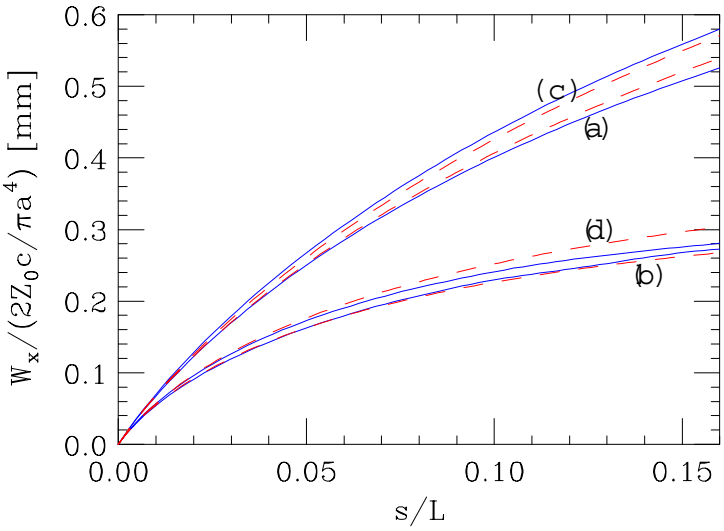

FIG. 5: Results of our parameter study cont'd: The numerically obtained wakefields (solid) and the result of the model Eq. 15 for 4 representative geometries studied in Fig. 4. Note that in this plot the wake has been normalized by $2Z_0c/(\pi a^4)$.

period length is $L = 8.75$ mm. It is a detuned structure (the modes of the first dipole band are Gaussian detuned), and the cell geometry gradually changes from beginning to end (the distributions in a and g are roughly Gaussian). For representative cells (1, 51, 103, 154, 206), a = (5.9, 5.21, 4.92, 4.66, 4.14) mm, g = (7.49, 7.09, 6.89, 6.70, 6.29) mm. All cells are within the parameter range of validity of our model. In Fig. 6 we display the numerical results for the different cell geometries (solid lines) and the model result (the dashes), and we see that the agreement is good. In this plot we also give the much earlier obtained results, using field matching at real frequencies plus the S-V extension, that were given in Ref. [1] (dots), and we see that the agreement is also good. For the short-range wake, the wake of a structure is given to good approximation by the average of the wakes corresponding to the geometry of the individual cells. In the plot we show, in addition, the average of the numerical results and the average of the model results for the five representative cell geometries (using trapezoidal rule). It turns out that the averaged wake here is about the same as one obtains by taking s_0 as given for the average cell (cell 103), increasing it by 7%, and inserting it into the model formula.

The second example structure is the 54-cell h50vg3 structure, an x-band structure that operates at $5\pi/6$ phase advance. The period length is $L = 10.93$ mm. The structure is also Gaussian detuned. For representative cells (1, 14, 27, 40, 54), a = (5.49, 4.94, 4.70, 4.46,

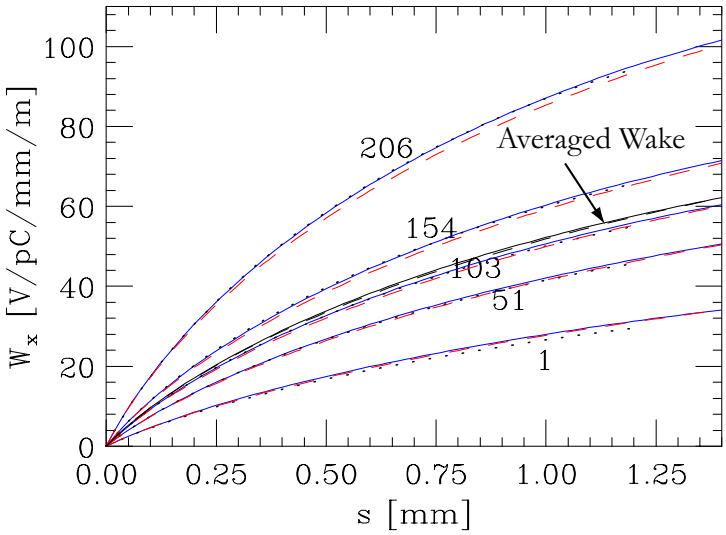

FIG. 6: Wakefield of representative cell locations within the DDS structure. Shown are numerical results obtained here (solid) and the results of the fitted model (dashes). Also shown are numerical results obtained by field matching with k on the real axis plus the S-V extension, and given in note NLC9 (the dots).

3.93) mm, g = (6.33, 6.75, 6.94, 7.12, 7.55) mm. Again all cells are within the parameter range of validity of our model. In Fig. 7 we display the numerical results for the different cell geometries (solid lines) and the model result (the dashes), and we see that the agreement is again good. Here the averaged wake is approximately the same as is obtained by taking s_0 as given for cell 27, increasing it by 12%, and inserting it into the model formula.

The final example, the SLAC main linac structure—which is not an NLC linac structure—is another test of the model. The SLAC structure operates at s-band, at $2\pi/3$ phase advance, and the dipole modes are linearly detuned (the iris radius a varies linearly). The structure period $L = 34.99$ mm and gap $g = 29.15$ mm. For cells (1, 23, 45, 65, 84), a = (13.11, 12.44, 11.63, 10.73, 9.62) mm. Of these representative cells, note that only cells 1 and 23 are within the parameter range of validity of our model. Nevertheless, the agreement between model and numerical result is still relatively good. Here the averaged wake is about the same as is obtained by taking s_0 as given for cell 45, increasing it by 10%, and inserting it into the model formula.

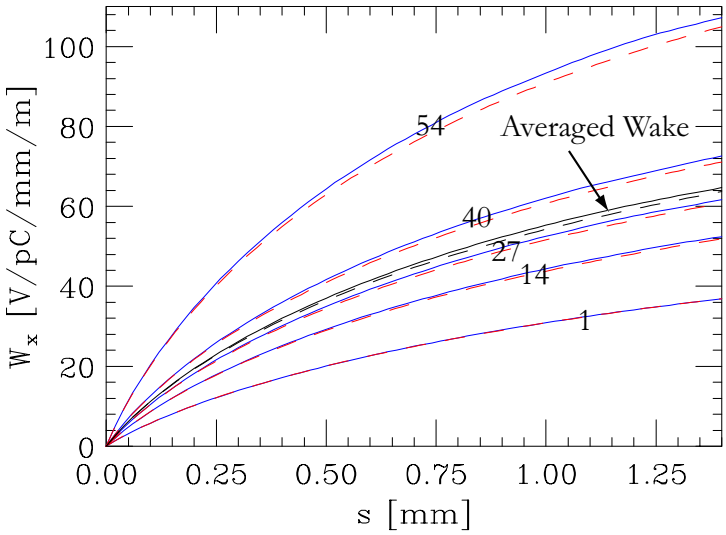

FIG. 7: Wakefield of representative cell locations within the h60vg3, $5\pi/6$ structure. Shown are numerical results obtained here (solid), and the results of the fitted model (dashes).

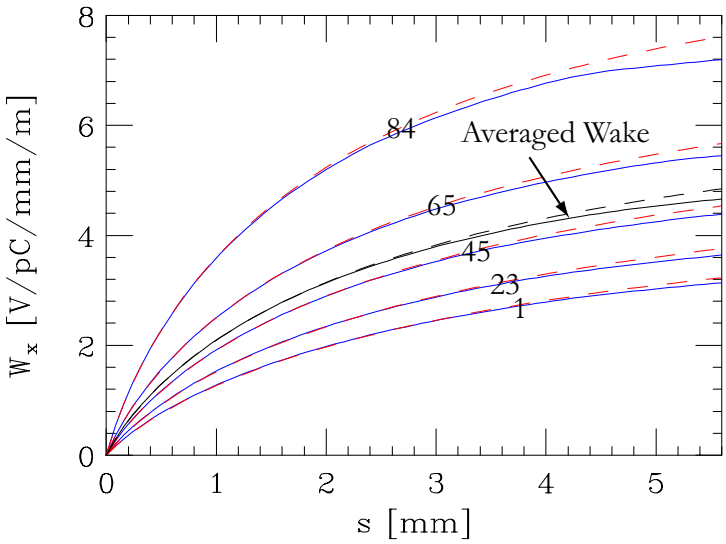

FIG. 8: Wakefield of representative cell locations within the SLAC linac structure. Shown are numerical results obtained here (solid), and the results of the fitted model (dashes).

Acknowledgments

The author thanks K. Yokoya for discussions about this problem and for providing his computer program that was used in this work. This work was supported by the Department

of Energy, contract DE-AC03-76SF00515.

---

[1] K. Bane, SLAC-NLC-Note 9, SLAC (1995).

[2] K.L.F. Bane, A. Mosnier, A. Novokhatsky, K. Yokoya, in *Proceedings of the 1998 International Computational Accelerator Physics Conference (ICAP98), Monterey, CA* (Stanford Linear Accelerator Center, Menlo Park, CA, 1998).

[3] K. Yokoya, KEK-Report 90-21, KEK (1990).

[4] K. Yokoya, *Short range wake formulas for infinite periodic pill-box* (1998), unpublished.

[5] A. W. Chao, *Physics of collective beam instabilities in high energy accelerators* (John Wiley & Sons, New York, NY, 1993).

[6] R. L. Gluckstern, Physical Review D **39**, 2780 (1989).

[7] K. Yokoya and K. Bane, in *Proceedings of the 1999 IEEE Particle Accelerator Conference, New York, NY* (Piscataway, NJ, 1999), p. 1725.

[8] A.V. Fedotov, R.L. Gluckstern, M. Venturini, Physical Review Special Topics–Accelerators and Beams **2**, 064401 (1999).

[9] H. Henke, Particle Accelerators **25**, 183 (1990).

[10] K. Bane and P. Wilson, in *Proceedings of the 11th International Conference on High Energy Accelerators, Geneva, Switzerland, 1980* (Birkhäuser Verlag, Basel, Switzerland, 1980), p. 592.

[11] K. Bane and B. Zotter, in *Proceedings of the 11th International Conference on High Energy Accelerators, Geneva, Switzerland, 1980* (Birkhäuser Verlag, Basel, Switzerland, 1980), p. 581.

[12] E. Keil, Nuclear Instruments and Methods **100**, 419 (1972).

[13] I. Zagorodnov and T. Weiland, in *Proceedings of the International Computational Accelerator Physics Conference 2002, Lansing, MI (ICAP-2002)* (2002).